EFFECTS OF SALINE CONDITIONS ON THE SOIL POROSITY IN THE CHELIFF VALLEY, ALGERIA

Djamel. Saidi*, Y. Daoud** and Mahmoud A. Essa***

* Faculty of Agriculture and Biology Sciences, Chlef University, Chlef, Algeria
** National Agronomic Institute, Department of Soil Science, El-Harrach, Algiers Algeria
*** Geology Dept., Faculty of Science, Assiut University

ABSTRACT:

Porosity variations of the saline and sodic clay soil have been studied by several approach methods (mercury porosity, final infiltration, water retention and microscopic observation). The main results showed that the stress saline conditions permitted to increase the total poral volume (V_T) of aggregations. Indeed, a saline constraint of the exchange sodium percentage (ESP) of 52.5% caused an increase in the total poral volume of 63.4 %. The distribution curves of pore diameter resulted in the existence of three different poral volumes of V_A, V_B, V_C, corresponding to the structural, lacunar and clay pores, respectively. The results showed also that both the structural porosity and lacunar porosity were linearly related to the ESP. This was not the case for the clay porosity, which decreased with increasing the soil salinity and sodicity. The results of the influence of the ESP on the evolution of the poral volumes showed that below an ESP level of 11%, the poral volume decreased in the order of $V_C > V_A > V_B$. However, above this ESP level, the tendency reverses resulting in an order of $V_A > V_B > V_C$ and a stabilization in the final infiltration level of the soils corresponded to a complete extension of the sedimentary crust.

The micromorphological observation of the thin section makes easier the interpretation of the poral space, provides first the essential information concerning the microstructural organization at the aggregate level with its regular assembly, and then develops the mechanisms of disintegration until the reorganization to the level of the massive aggregation with formations of microhorizons. The main feature is that the presence of a structural poral space under saline conditions does not necessarily make sure a more elevated level of infiltrability because it can function very well only by the textural pores or by the cracks of climatic origin. The clay phase is abundant; its poral volume decreases in regard to the other pore volumes; it is due to the role of the sodium in the clay particle division, which causes an increase in the number of the contact surface that is responsible of fine particle assemblies with the skeleton.

INTRODUCTION:

The analysis of the soil porosity frequently rests on the hypothesis that one can distinguish two different origin pore compartments (Stengel, 1979; Monnier and Stengel, 1982).

The structural porosity results from the action of outside agents (climatic factors, living

organisms and frameworks), while the textural porosity comes from the elementary particle assembly. One generally considers that the textural porosity is a function of the elementary particle nature (granulometry and mineralogy) and is of a hydric state.

This textural porosity can be decomposed in two coin compartments (Fiès and Zimmer, 1982; Fiès, 1984): the lacunar porosity that has a dimension closer to the one of the slimy or sandy skeleton and this porosity is owed to the assembly of the clay phase with grains of the skeleton, and the porosity of the clay phase which results from the fine particle assembly between them.

When a soil is submitted to the saline stress, both structural and textural porosity compartments are affected in a different way. At the microscopic and macroscopic scales, the porosity of soils is dependent of the clay fraction and the history of the constraints undergone by soils (Halitim *et al.*, 1984; Tessier, 1984; Bruand *et al.*, 1988 ; Bruand, 1993), except in the case of sandy soils (Coulon and Bruand, 1989) and certain silty loam soils (Grimaldi, 1986), where the textural compartment is not generally modified.

With regard to clays, Halitim and al., (1984) showed in particular that a sodic constraint having ESP (Exchange Sodium Percentages) of 10 to 80% provokes an increase in the porosity of Wyoming montmorillonite of 0.5 % to 18%.

The main objective of this work is to surround variations of poral spectre of the Cheliff plain soils which are made of silty clay loam texture and which show extremely variable saline conditions. Variations of the porosity and the distribution of the pore sizes are studied by an analysis in porosimetry to mercury and are compared to the microscopic observations and the measurements of the hydric behaviour.

MATERIALS AND METHODS:

1-Site:

This research was conducted in the Mina area (lat. 36°-10' N, long. 00°-30' & 1°-20'E) of lower Cheliff Valley, Algeria (Fig. 1). The specific climate is semi-arid with very hot summer and low temperature winter. The mean annual rainfall of this area is 350 mm and the mean annual temperature is 18.40°C with only major fluctuations through the year. The altitude at this plain is about 70 m above the sea level and the parent material of the soil is alluvium. The studied soils are pedologically young and developed from a rich clay calcareous material (Boulaine, 1957; Saidi, 1985). The soil particles that have a diameter < 2μm are mainly illites accompanied by a mixture of clay minerals of smectite, kaolinite and chlorite. These soils represent a strong structural instability (Saidi, 1992).

The sampling has been achieved in order to cover a large range of salinity (expressed by the electric conductivity of the saturated soil past in dS/m at 25°C, ECe) and the point of view of the sodicity (expressed by the exchangeable sodium percentage, ESP).

2-Soil:

Soil samples were collected from the upper layer of the Mina fields in the Cheliff plain, Algeria. A total of seven (7) samples were taken from the surface horizon (0-30 cm) of each cultivated soil and analyzed using the standardised methods. The granulometric analysis was carried out without the decalcification after the dispersion with sodium hexametaphosphate. The percentage of organic carbon is given according to Anne method; the soil pH is measured in a 1:2.5 ratio of a soil to distilled water suspension. Total calcium carbonate is obtained by Bernard volumetric

calcimeter. The specific surface was measured by the adsorption of Ethylene Glycol Mono Ethyl Ether (EGME) according to the protocol developed by Heilman *et al*. (1965). Both cation exchange capacity and exchangeable cations at the pH of the soil were determined by using the solution of cobalt hexamine (Cohex) trichloride, $[CO (NH_3)_6]Cl_3$, (Ciesielski *et al*., 1997) in an accredited analysis laboratory of INRA, Arras, France. All these methods are standardized (standards AFNOR, 1996).

Fig. (1): Location of the studied area (Encarta, 2007)

3-Preparation of thin sections:

The non perturbed natural samples appropriated to the surface of soil with shape clods have been air-dried and impregnated with a polyester resin that is diluted to 30% by the styrene. This technique is used to make thin sections according to the method of Guilloré (1980). The thin section achieved measurements are 45 mm X 60 mm; they are non polished and non covered. These thin sections are studied on the basis of photogram to a level of organization accessible to the polarizing optic microscope.

They are described according to Bullock et al., (1985).

Five microstructures presenting the descriptive and identification features of the structural organization states of soils were carried out in samples of the Cheliff. Among them, two microstructures of the crust (structural crust and sedimentary crust) of saline and sodic soils are illustrated.

4-Mercuric porosimetry:

The porosity of these clods has been also studied in Mercuric porosimetry (Murphy *et al*., 1977; Vachier *et al.,* 1979; Fiès, 1984;

D'Acqui *et al.,* 1994). Measures are applied on fragments of massifs dried in desiccators during 24 h to 105 °C and forced through sieving mesh to get aggregations weighing about 1.5 g.

The used device is a porosimetry of Micromeritics Pore Sizer 9310 type, permitting to exercise a pressure of an intrusion varying from 0.003 to 200 MPa, which is corresponding to the equivalent diameters of 0.006 to 400 μm. The angle of mercury adjusting is fixed to 130° and the superficial tension to 4.84 N m^{-1}. Every analysis has been programmed to permit to do 53 intrusions of mercury.

Mercury is a liquid not wetting, forming to the contact of most of the mineral materials an adjusting angle superior to 90°. The introduction of mercury in the porous materials is made, therefore, by an application of a certain pressure (P), by assimilating a pore to a capillary; the exerted pressure to fill this one is given by the law of Laplace:

$$P = 4\gamma \cos(\alpha/d)$$

P = applied or exerted pressure.
γ = superficial tension of mercury.
α = contact angle between mercury and pore side.
d = pore diameter.

An increase in the pressure allows the mercury to penetrate in the larger and smaller diameter pores. The mercuric porosimetry permits, thus, to determine the volume of pores as a function of their equivalent diameter. Measurements have been achieved into two repetitions.

5-Water Retention:

The determinations of water retention were related to fragments of centimetre size (5-10 cm^3) that were obtained by hand fragmentation. The apparent density of the fragments was measured using a petrol method (Monnier *et al.*, 1973; AFNOR, 1996). Two water contents were given for metric potential values of -330

hPa (W2.5 with pF=2.5) and of -15000 hPa (W4.2 with pF=4.2). The measurements were carried out using pneumatic devices. This device is connected with that used by Tessier and Berrier (1979) by making it is possible to put at balance 30 to 40 mounds at the same time in only one cell. The water content is measured after 7 days of setting to the balance with the selected pressure and then, a passage to the drying oven with 105 °C during at least 24 h.

6-Measurement of the soil infiltration under simulated raining:

a-The rainfall simulator:

The artificial rains were implemented using a sprinkling device. The rain simulator is established according to the model designed by Asseline and Valentine (1978). It consists of a watering system fixed at a pyramidic tower of 4 metres in height and protected from the wind action by a removable cover. Sprinkling is ensured by a metering jet (tube n° 6540) assembled on an oscillating arm whose movement is printed by an electric motor. This infiltrometer with sprinkling makes it is possible to simulate rains of controllable intensities on a measurement seat. The range of available intensity varies from 20 to 150 mm/h. The protocol of simulation includes several rain tests of an average intensity of 30 mm/h (±2 mm.h^{-1}) during one hour and half, and 45 mm of precipitation. It well corresponds to that met in the zone of the study for a natural rain event of decennial recurrence. The water flux through the sample was measured every 5 min, and the ratio between the final infiltration and the rainfall (the final infiltration coefficient) was calculated for the experiment. The treatments were replicated three times for each soil.

b-Preparing the samples:

Twelve distant samples of approximately 10 cm are distributed on a PVC plate measuring

50x50 cm. The soil samples of a volume of 78.5 cm^3 resting on a bed of 1 cm of calibrated and washed sands are put in cylinders made of PVC of 5 cm in diameter and 5 cm in height. They are transparent in order to be able to visually control the moistening. They are perforated at their bases to be used as holes of evacuation for the infiltration measurement. The soils are initially saturated by the base. Then, they are exposed to a rainfall simulated by using distilled water until the rate of the stabilized infiltration is obtained. The standard conditions of the simulator operation for each episode rain are calibrated and checked. The analysis of each group of data primarily relates to the evaluation release time of the infiltration and, thereafter, to the measurement of the water volume infiltrated for each rainy event.

RESULTS:

1-Characteristics of soil samples :

The physical and chemical characteristics of the seven studied soils are given in Table 1. The soils are of basic pH and generally calcareous, with contents of organic matter ranging between 0.53 and 3.35% and a clay loam texture with clay content higher than 40%. The electric conductivity of the saturated soil paste (ECe) varies between 1.93 and 41.33 dS/m. The exchangeable sodium percentages of the samples destined to the survey of the porosity and the physical behaviour vary from 3.3 to 52.5% ESP. Values of the CEC of the soils using the cobaltihexammine trichloride method vary from 17.1 to 20.8 Cmol$_c$/kg. The soil fraction having a diameter lower than 2 µms belongs to the facies characteristic of illitic with a mixture of clay minerals of smectite, kaolinite and chlorite (Saidi, 1993). The specific area of the clay fraction varies from 310 to 360 m^2/g.

2-The microscopic observations:

The thin section observations in the optic microscopy permitted to describe the organization of the microstructure that translates the distribution and the localization of the microphone aggregations to the strong matrix, the assembly of aggregations and shapes of porosity.

An aggregation of the soil that is constituted by an assembly of several aggregations of smaller size is observed in Figures (2a &2b). This assembly is oriented in a regular way according to the size of microphone aggregations. The observation reveals the existence of pores whose morphological features are bound to the initial aggregation size. A more heterogeneous size distribution will drive to a more compact assembly.

Table (1): physical and chemical properties of the studied samples

Sample	Clay (%)	Silt (%)	Sand (%)	Specific area (m^2/g)	Organic matter (%)	pH	CEC (Cmolc/kg)	CaCO$_3$ (%)	ECe (dS/m)	ESP (%)
	46	35	19	325	3.38	8.24	20.2	20.9	1.93	3.3
MII	44	41	15	324	1.95	8.15	17.7	20.7	3.83	5.0
MIII	44	42	14	321	2.54	8.15	17.1	19.6	4.25	8.2
MIV	47	38	15	335	1.90	8.00	20.8	17.5	18.41	11.3
MV	43	41	16	316	2.37	8.20	18.5	19.4	20.70	27.2
MVI	41	45	14	310	2.30	8.03	19.3	22.1	32.53	40.4
MCR	45	46	9	360	0.53	8.33	19.7	8.0	41.33	52.5

The microscopic observation reveals that the aggregations are fissured and the cracking is dense, clearing different size fragments (Figs. 3a and 3b). The cracking is about a severance of the skeleton and the plasma within aggregations was bound to the contact between water and the earthy fragments at the time of the brutal humiditation.

Figures (4a&4b) indicate the presence of bladders and the sinuous paths within the earthy fragment. They are about a detachment of fragments of small size aggregations that creates the interconnected emptiness and constitutes the porosity in fairway. In addition, the pores inter aggregations are plugged by fine particles or by accumulated salts.

Under the action of rain, the structure of the superficial layer evolves toward a structural crust formed by a more important interstitial plugging and the coalescence of fragments and, in some parts disconnected quartz are accumulated (Figs. 5a &5b). The presence of microhorizons represented by alternated accumulations of fine and coarse particles is observed under strata shapes (stratified organization) as it is shown in Figures (6a & 6b).

This shape reveals that the surface has reached a state of deterioration with forming a deposit crust. This deposit, in superimposed stratum, suggests that it represents the origin of the suspension, the transportation and the deposit in liquid phase of various sizes solid particles (Chen, 1980; Valentin, 1981; Boiffin and Bresson, 1987; Le Bissonnais, 1988). Some aggregations of small size having preserved structure were observed with depth but they are welded practically by fines. The microscopic observation in the polarized light permits to differentiate between emptiness pores and the salt accumulations. The solid saline phases are localized in the interstices of the recess cracks, the fissuring and the clay plasma.

3-Mercury porosimetry:

The mercury porosimetry shows an increase in the total poral volume (V_T) of aggregations with increasing the constraint of the saline phase (Table 2). The total poral volume (V_T) increases from 11.59 to 63.38% with increasing the exchangeable sodium percentage (ESP) from 5.05 to 52.50%.

Table (2): Total poral volume (V_T) and elementary poral volumes (V_A, V_B and V_C) determined in mercury porosimetry on aggregations of soils submitted to the saline constraints.

Saline Constraints		Distinct poral volumes						Total poral volume	
Salinity (Ece)	Sodicity (ESP)	V_A		V_B		V_C		V_T	
dS/m	%	cm³/g	%	cm³/g	%	cm³/g	%	cm³/g	%
1.93	3.27	0.044	25.04	0.037	20.87	0.095	54.14	0.175	0.00
3.83	5.05	0.058	29.71	0.047	24.08	0.090	46.21	0.195	11.59
4.25	8.2	0.062	31.96	0.049	25.06	0.084	43.03	0.194	11.07
18.41	11.24	0.077	35.52	0.056	26.09	0.083	38.39	0.216	23.59
20.7	26.7	0.099	41.05	0.063	26.26	0.079	32.70	0.241	37.60
32.53	39.6	0.111	41.22	0.094	34.80	0.065	23.98	0.270	54.23
41.33	52.5	0.134	47.03	0.105	36.63	0.047	16.34	0.286	63.38
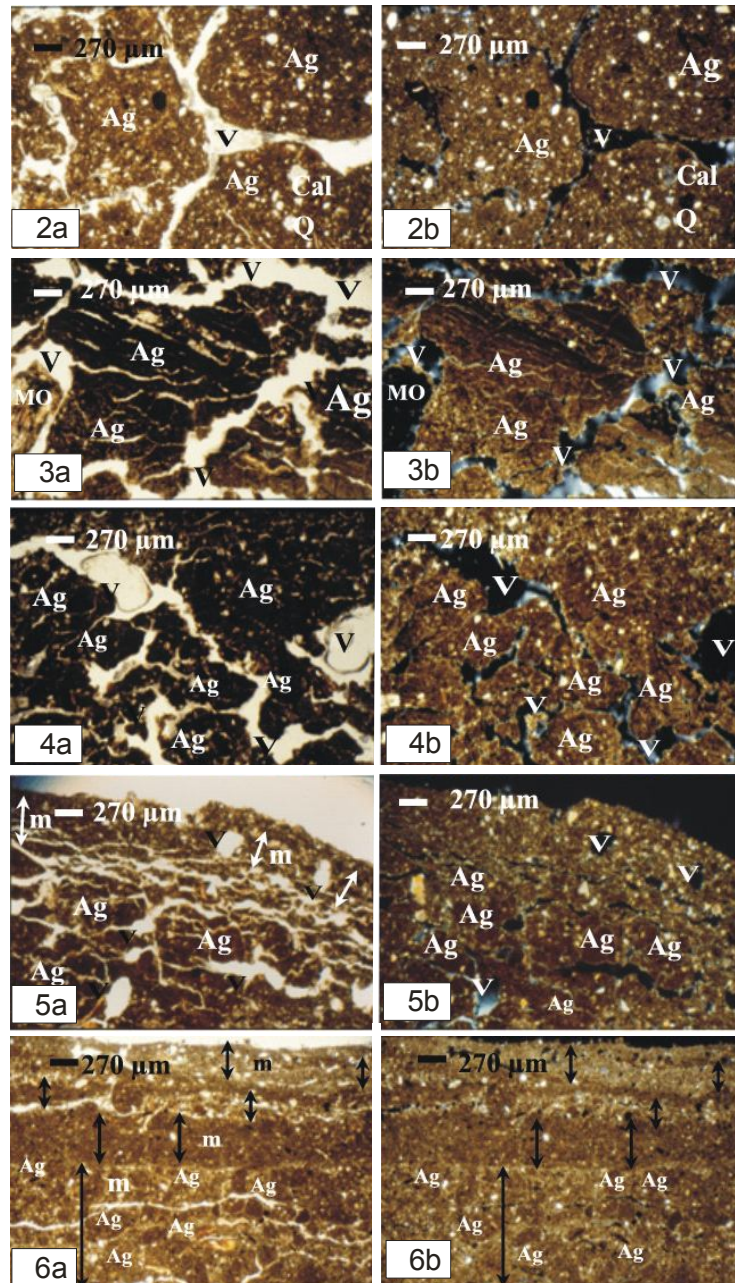
The microstructure of the soil and the composition of the surface layer
Fig. (2): Photomicrograph of the microaggregate assemblages.
Fig. (3): Photomicrograph of the microstructure of fragments.
Fig. (4): distribution of microaggregates and formation of pores structures.
Fig. (5): Characteristics of microhorizon of the structural facies.
Fig. (6): Microhorizon characteristics of the sedimentary facies.
a: observation in ordinary light , b: observation in polarized light.
Ag: microaggregate; V: void of pore; Q: quartz; Cal: calcite
MO: Organic matter; ↕ m: microhorizon.

The mercury porosimetry provides the poral spectre of dehydrated samples. Curves of mercury intrusion clearly appear the existence of three distinct pore volumes (V_A, V_B, V_C) corresponding to three successive entries of mercury (Fig. 7). For clods coming from zones presenting different states of salinity and sodicity, these three pore volumes are interpreted according to Bruand *et al*., (1993) corresponding to the structural, incomplete and clay poral volumes, respectively. The analysis of distribution curves indicates that the structural poral volume is accessible to diameters of constriction taken between 320 and 5.6μm, the incomplete poral volume gets into diameters of constriction taken between 5.6 and 0.18μm, and the poral volume of the clay phase is accessible to diameters of constriction taken between 0.18 and 0.006μms. These values are close to those recorded by Bruand and *et al*. (1993).

Figure (8) shows that both structural and lacunar porosity increase whereas the porosity of the clay phase decreases with the salinity. At an ESP value lower than 11.24%, the structural porosity is lower than the porosity of the clay phase. However, the opposite is for ESP values superior to 11.24%.

The structural poral volume increases from 25.04 to 47.03% and the lacunars poral volume increases from 20.87 % to 36.63% when the sodicity (ESP) increases from 5.05 to 52.50% and the salinity (ECe) increases from 4.25 to 41.33 dS/m (Table 2). On the other hand, the porosity of the clay phases decreases from 54.14 to 16.34 % under the same sodicity and salinity conditions.

It appears that at the less severe saline conditions (ECe < 18 dS/m and ESP < 11 %) the porosity of the clay phase is more important than the structural and incomplete porosity according to the decreased order of $V_C > V_A > V_B$. On the other hand, it becomes less important where the order is $V_A > V_B > V_C$ when salinity and sodicity constraints become very severe (ECe > 18 dS/m and ESP > 11 %). These results lead to propose a threshold, in terms of ESP and ECe to characterize the organization of the structural state of the soil.

4-Water retention:

Comparing the results of the porosity analysis gotten from mercury porosimetry with the results of water contents at pF=2.5 and pF=4.2 for the natural samples at different sodicity levels. Figure 9 shows that the water retention at pF=2.5 is proportional to the total poral volume, which is not the case for the water retention at pF=4.2. However, the water content at pF=4.2 increases with the poral volume of the clay phase (Fig. 10) and therefore, with decreasing the exchangeable sodium percentages. At pF=2.5, the water retention properties depend on the geometry of pores within the structural and lacunars porosity. On the other hand, at pF=4.2, the water retention depends on the poral volume of the clay phase as well as the mineralogical nature and sodicity.

5-Regime of infiltration:

In order to be able to compare regimes of infiltration, we represented them according to the ESP with the help of a power relation.

$$\hat{I}_{(f)} = \alpha \, x^{-\beta} \, ; \, \beta > 0.$$

Where î (f) is infiltration estimate; x is the value of the ESP and α β are constants that indicate the final infiltration at ESP value of 1% and the regime of the final infiltration rate decreases according to the ESP. To evaluate the streamlined behaviour of surface, it is useful to use the rate of β decrease which is much higher than the infiltration decrease. This β parameter could be used as diagnosis criteria of the soil behaviour in situ. The obtained infiltration curve (Fig. 11) presents a reduction marked for

the low ESP values. It reaches then a plateau, whatever is the value of the ESP.

The analysis of this curve, established on soils of different salinity and sodicity levels, indicates that under the conditions one supposes that it is less severe (EC < 18 dS/m and ESP < 11%), the regime of final infiltration decreases 50%. There is an influence of the clean resistance of aggregations and therefore, the action of rain, on lowering the final infiltration of the layer. This decrease intervenes during the starting point of the scattering process at the time of the disintegration. Under the severe conditions, the final infiltration decreases 60% and stabilizes at 63%. In this case, the limit in these two phases coincides distinctly with an ESP value of 11%, whereas beyond it, the curve reaches a plateau.
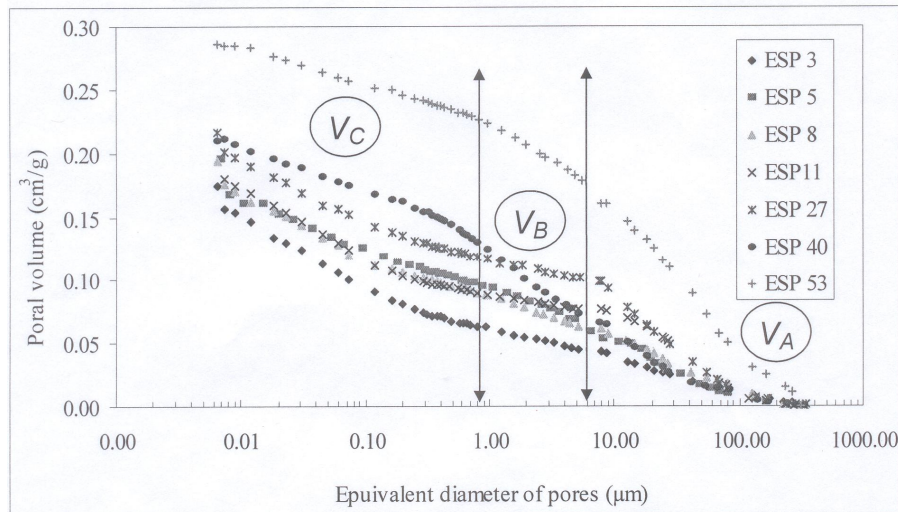

Fig. (7): Distribution of accumulated poral volume, obtained in mercury porosimetry, with aggregations of different saline phases, in terms of the equivalent diameter of pores
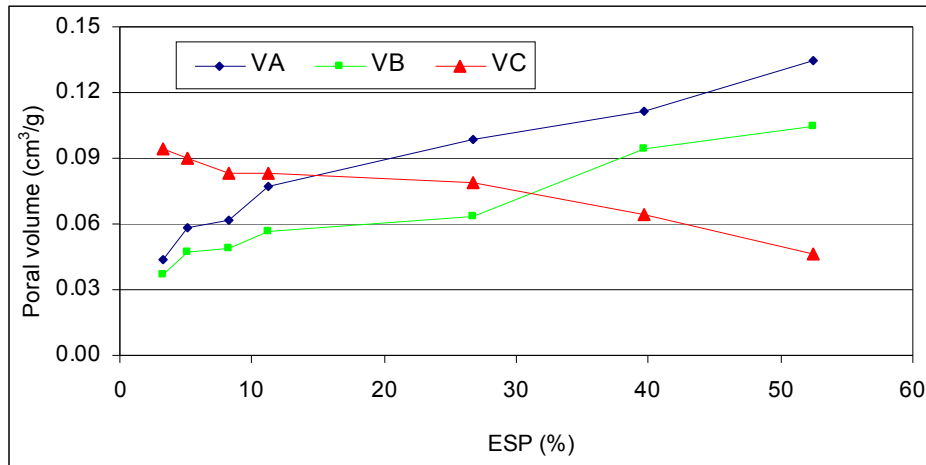

Fig. (8): Relation between poral volumes of materials affected by the exchangeable sodium percentages (ESP).
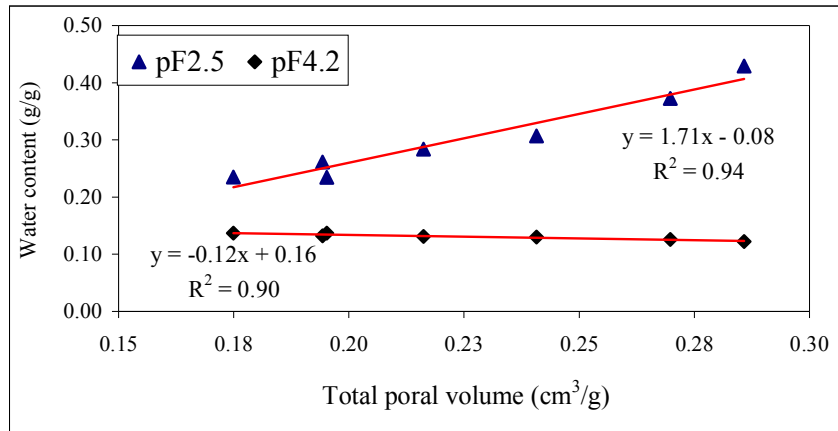
Fig. (9): Relation between the porosity and the water content in the clay material at different salinity and sodicity levels. Examples of regression models for -330 hPa and - 15000 hPa.
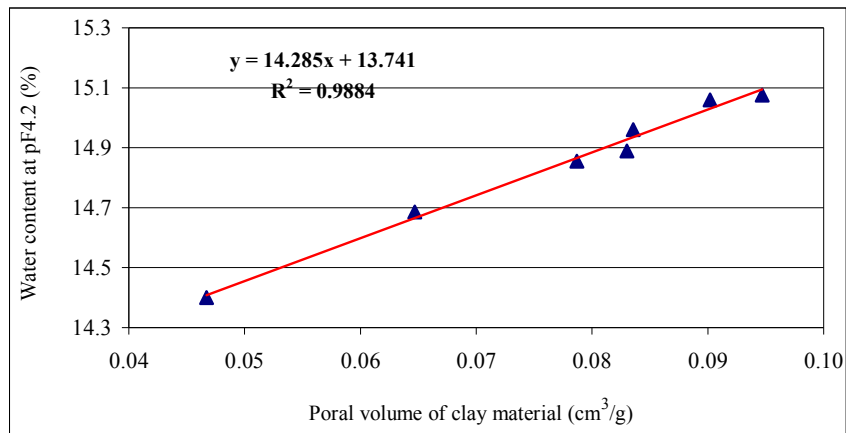

Fig. (10): Relation between poral volume (VC) and the water content in the clay material at different salinity and sodicity levels. An example of regression model for -15000 hPa.
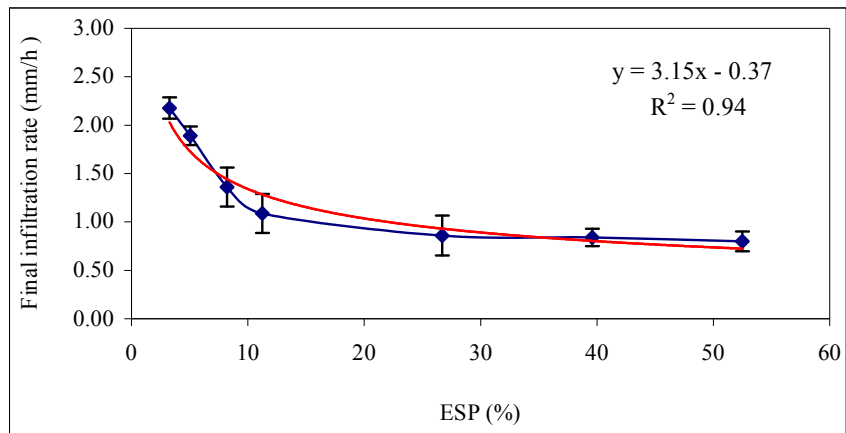

Fig. (11): Influence of the exchangeable sodium percentage (ESP) on the regime of the final infiltration rate

DISCUSSION:

The adopted methodological procedure, during this study, reposes on the hypothesis that the poral space of a soil is composed of three whole of pores of different origins.

The observable empty spaces have variable size and morphology resulting in the structural porosity, lacunars porosity and the porosity of the clay phase. The last one mainly reflects the control of the physical state of the cultivated soils (Stengel, 1979). The clay phase is sufficiently abundant in the soils of the Cheliff valley to assure the continuity among grains of quartz. The thin pores result from the assembly of the clay phase and grains of quartz; they correspond to the incomplete emptiness defined by Fiès (1984) and Ouattara (1994). The other pores that have a bigger size result, at least partially, from the assembly of aggregations and from the climatic influence (fissuration). However, neither their size, nor their morphology permits to discuss their origin with precision. These pores that delimit the structural elements (Figs. 2a and b) lead to the structural porosity. The qualification makes reference to a particular scale of the structure (Monnier and stengel, 1982).

The saline condition influence in the soils of arid and semi arid regions generates a volume of supplementary pores of lacunars and structural origin. Lacunars pores that come from the interaction clay skeleton are not reparable to the optic microscopy. However, the structural pores develop fissures or micro fissures that are located in Figures 5 a, b and 6 a, b and called the fissure porosity or drying porosity.

The quantitative results of the soil poral analysis show that each of these three groups of pores, with various degrees, is susceptible of deep modifications, with the saline conditions.

The simple correlation permits to identify the connection level of certain studied parameters (Table 3). The correlation coefficients are very close and are over 0.78.

Positive strong links between the water retention at the field capacity and the structural poral and lacunars volume. Moreover, the poral volume of the clay phase (V_C) is very strongly correlated to the water content at the field capacity (r = -0.99).

The water retention, which translates the affinity of the soil sample for water and inform on the localization of water at the time of the extraction, can be analyzed and represented (Tessier, 1984; Bruand, 1986; Bruand *et al.,* 1988). At water retention of -330 hPa, the structural reorganization influences considerably the water retention. Indeed, during the soil salinization and the sodization, the poral volume increases. Using the total water potential, expressed as a pF value that is equal to the sum of the matrix potential and the osmotic potential (Hillel, 1984), one can expect that the increase in the osmotic potential has the same effects on the total poral volume.

At some water retention of -15000 hPa, the increase in the constraint results in a distortion of the material and a reduction in the emptiness size. Indeed, the curve of water content in regard to the total poral volume is reversible.

The water content varies, however, linearly with the porosity of the clay phase with a correlation coefficient of r=0.98. Thus, the suction has a big influence on the clay material microrganization (Halitim *et al*., 1984).

The poral volume of the clay phase (V_C) is developed in an inverse way to the soil salinity and sodicity. If one compares the two extreme ESP values of 52.5 to 3.27%, which means to compare the retention of the sodic clay phase to the calcic clay phase, the favourable influence of the calcium on water retention will be evident.

The calcium keeps a lot more of water than the sodium. The difference in the water content is a function of the cation hydration properties. The obtained results agree with those of Tessier (1981) and Halitim *et al*., (1984). Saline conditions seem to be accompanied, however, by a reduction in the porosity of the soil fine fraction; this influence is explained by the role that is played by the sodium ion in the scattering and the fine particle division (Halitim *et al*., 1984; Shainberg and Letey, 1984) and in the infiltration reduction, which strongly affects the closing of the surface state (Yousaf et al., 1987; Le Bissonnais, 1996).

The salinization and the sodization processes in the soils of Cheliff region, which cause a reduction in the aggregate structural stability, provoke a modification of the organization of the poral system of superficial horizon samples and the apparition of dandruff to the surface of the soil under the impact of rain drops (Figs. 5 a, b and 6 a, b). These two processes can explain the closing of the surface state.

The regime variation of the final infiltration rate of the studied samples during the downpour (Fig. 10) shows the sequence of two phases. The first phase corresponds to the less severe conditions (ECe < 18 dS/m and ESP < 11%) where the final infiltration rate decreases progressively. The second one shows that the regime of the final infiltration rate evolves slowly until a stability limit. The marked decrease phase ends at the complete extension of the crust as it was suggested by Baumhardt *et al*., (1990). There is, in this case, simultaneity between the extension of the crust and the decrease in the infiltrability.

The severe saline conditions strongly influence the hydrodynamic behaviour of the aggregation mass. The evolution of the infiltration in the saturated regime, under the saline conditions agrees itself with the evolution of pore volumes and then with the reorganization of the surface of the mass which coincides distinctly with the closing of the surface state.

The micromorphological study of this aspect shows the individualization of several superimposed microhorizons. This organization is typically the one of structural crusts (Figs. 5 a, b) and of the sedimentary crusts (Figs. 6a, b). They have been described and have been characterized by Valentin (1981) and Casenave and Valentin (1989). These authors put in evidence that the evolution of the infiltration regime depend mainly on reorganizations of surface.

Table (3): Linear correlation coefficients between the saline phase (ECe and ESP), the porosity, water retention (PF2.5 and PF4.2) and the final infiltration rate (IF).

	ECe	*ESP*	V_T	V_A	V_B	V_C	$pF_{2,5}$	$pF_{4,2}$	I_F
ECe	1.00								
ESP	0.97	1.00							
V_T	0.98	0.98	1.00						
V_A	0.98	0.98	0.99	1.00					
V_B	0.97	0.98	0.98	0.97	1.00				
V_C	-0.95	-0.97	-0.95	-0.96	-0.98	1.00			
$PF_{2.5}$	0.98	0.99	0.97	0.97	0.99	-0.99	1.00		
$PF_{4.2}$	-0.96	-0.95	-0.95	-0.96	-0.96	0.98	-0.98	1.00	
I_F	-0.85	-0.80	-0.87	-0.88	-0.80	0.78	-0.81	0.88	1.00

CONCLUSION:

The results show that the limit between the structural porosity and the textural porosity is not as clear as one generally admits. By using the technique of mercury porosimetry, it will be recognized that the textural porosity contains two compartments, the internal porosity of the clay phase, whose pores have very small diameters and the lacunars porosity that is close to the silty or sandy skeleton. The lacunars are generated by the clay-skeleton interaction during the process of particle arrangement which determines the textural porosity.

During the severe saline conditions, modifications seem to be very local, but they deeply affect the behaviour of the structural, incomplete pores and the clay phase whose the majority of them is accessible in mercury porosimetry. Indeed, the structural and lacunars pores evolve progressively with the ESP, because they nearly develop the same volumes contrary to the pores of the clay phase.

The obtained results, for the clay loamy soils, suggest that because of their very weak structural stability to the humid state, the increase in the ESP provokes a fragmentation of the aggregations by slaking followed by the physical-chemical dispersion of the clay particles. These mechanisms are responsible for the increase in the incomplete and structural poral volumes. On the other hand, an inverse effect appears at the time of the increase in the ESP that provokes a clay particle division and therefore, a reduction in the poral volume of the clay phase. This clay porosity strongly affects the behaviour of samples with a preserved and studied structure.

Furthermore, the results of pore volumes show that before reaching a particular threshold, they decrease in the order of $V_C > V_A > V_B$ whereas when this threshold is passed, the tendency reverses itself and the structural poral volume becomes predominant as well as a stabilization of the final infiltration of soils. The ESP threshold of 11% permits to differentiate between soils with damaged structure and non damaged structure.

Thus, the evolution of the soil porosity permits to give information about the different mechanisms responsible for the structural and physical behaviour of soils. However, under the saline phase stress, distinct pore volumes influence the water retention and the hydrodynamic behaviour by inverse mechanisms.

One can notice that the essential character for properties of hydric transfer and storage necessitate the analysis of the pore continuity that requires the 3D knowledge on the pores network. Currently, other new techniques that use the tomography to study the connectivity of macropores in soils and fractales would permit to get some more precise information on 3D geometry of the network of soil pores.

REFERENCES:

AFES, (1995): Référentiel pédologique de France (RPF), Ed., INRA., 332 p.

AFNOR, (1996): Qualité des sols. Recueils de normes Française, AFNOR, Paris, France, 533 p.

Asseline, J. and Valentin C. (1978): Le simulateur de pluies de l'*ORSTOM*. Cahier Hydrologie de l'*ORSTOM*., Paris, V. 4, pp. 321-347.

Baumhardt, R. L.; Romkens, M. J. M. and Whisler, F.D. (1990): Modeling infiltration into a sealing soil. *Water Resour. Res*. V. 26, pp. 2497-2505

Boiffin, J. and Bresson, L.M.(1987): Dynamique de formation des croûtes superficielles: Apport de l'analyse microscopique. In: Micromorphologie des sols. Actes de la VII Réunion internationale de

Micromorphologie des sols, Paris, juillet 1985. Eds., AFES, pp. 393-399.

Bruand, A.; Tessier, D. and Baize, D. (1988): Contribution à l'étude des propriétés de rétention en eau des sols argileux: importance de la prise en compte de l'organisation de la phase argileuse, *Compte Rendu d'Académie des Sciences, Paris, série* II, V. 307, pp. 1937-1941.

Bruand, A.; D'acqui, L. P.; Nyamugufata, P.; Darthout, R. and Ristori, G. G. (1993): Analysis of porosity in a tilled "crusting soil" in Zimbabwe, *Geoderma*, V. 59, pp. 235-248.

Bullock, P.; Fedoroff, N.; Jongerius G.; Stoops, G. and Tursina, T. (1985): Handbook for soil thin section description. Waines research publication, Wolverhampton, U. K .

Casenave; A. and Valentin, C. (1988): Les états de surfaces de la zones sahélienne : Influence sur l'infiltration. *Ed. ORSTOM*, 230 p.

Chen, E.A.(1980): Scanning electron microscope observations of soil crust and their formation *Soil Sci,* V. 130, pp. 49–55.

Ciesielski, H. and Sterckemann, T. (1997): Determination of exchange capacity and exchangeable cations in soils by means of cobalt hexamine trichloride. Effects of experimental conditions, *Agronomie,* V. 17, pp. 1-7.

Coulon, E. and Bruand, A. (1989): Effects of compaction on the pore space geometry in sandy soils, *Soil Till. Res.,* V. 15, pp. 137-152.

C.P.C.S. (1967): Classification des sols. Laboratoire de géologie et de pédologie de l'ENSA de Rennes, Paris-Grignon 87 p.

Daoud, Y. (1993): Contribution à l'étude des sols des plaines du Cheliff. Le phénomène de salinisation, conséquences sur les propriétés physiques des sols argileux. Thèse de Doctorat d'Etat, INA, Alger, 233 p.

D'acqui, L. P.; Bruand, A. and Pagliai, M. (1994): Study of soil porosity with mercury porosimetry and image analysis on backscattered electron scanning images (BESI). Application to tilled "crusting soils" in Zimbabwe, 9th International Working Meeting on Soil Micromorphology, Townsville, Queens-and, Australia, 12-17/07/1992.

Fiés, J. C. and Zimmer, D. (1982): Etude expérimentale des modifications de l'assemblage textural d'un matériau sablo - argileux sous l'effet de pressions. Bulletin du GFHN, V. 12, pp. 39-54.

Fiés, J. C. (1984): Analyse de la répartition du volume de pores dans les assemblages argile squelettes : Comparaison entre un modèle d'espace poral textural et les données fournies par la porosimétrie à mercure, *Agronomie,* V.4 (9), pp. 891-899.

Fiès, J. C. and Panini, T. (1995): Infiltrabilité et caractéristiques physiques de croûtes formées sur massifs d'agrégats initialement secs ou humides soumis à des pluies simulées. Agronomie, V. 15, pp. 205-220.

Grimaldi, M. (1986): Modifications structurales d'un matériau limoneux soumis à un compactage dynamique, *Science du Sol*, V. 24, pp. 269-284.

Guilloré, P. (1980): Méthode de fabrication mécanique et en série des lames minces. INA, Paris – Grignon, 22 p.

Halitim, A.; Robert, M.; Tessier, D. and Prost, R. (1984): Influence de cations échangeables (Na^+, Ca^{2+}, Mg^{2+}) et de la concentration saline sur le comportement physique (rétention en eau et conductivité hydraulique) de la montmorillonite. *Agronomie,* V. 4, pp. 451-459.

Heilman, M.O.; Carter, O.L. and Gonzalez, C.L. (1965): Ethylene glycol Mono Ethyl Ether for determining surface area of silicate minerals, *Soil Sci*ence, V. 100, pp. 356-360.

Hillel, D. (1984): L'eau et le sol. Academic Press, New York, 288 p.

Le Bissonnais, Y. (1988): Analyse des mécanismes de désagrégation et de la mobilisation des particules de terres sous l'action des pluies. Thèse Doct. de Science de la Terre. Univ. Orléans 196 p.

Le Bissonnais, Y. (1996): Aggregate stability and assessment of soil crustability and erodibility. I. Theory and methodology. European Journal of Soil Science, V. 47, pp. 425-437.

Monnier, G. And Stengel, P. (1982): Structure et état physique du sol. Encyclopédie des Techniques Agricoles, Fasc. 1140 et 1141, Editions Techniques, Paris.

Murphy, C. P.; Bullock, P. and Turner, R. H. (1977): The measurement and characterisation of voids in soil thin sections by image analysis. Part I. Principles and techniques, Journal of *Soil Science*, V. 28, pp. 498-508.

Ouattara, B. (1994): Contribution à l'étude de l'évolution des propriétés physiques d'un sol ferrugineux tropical sous culture: pratiques culturales et états structuraux du sol. Thèse de doctorat d'ingénieur, Université nationale de Côte d'Ivoire; 156p.

Saidi, D. (1985): Etude agropédologique de la plaine de la Mina (Relizane) et évaluation des propriétés physiques des sols. *Thèse Ing., INA.,* Alger 80 p.

Saidi, D. (1992): Etude expérimentale de la stabilité structurale des sols des plaines du Cheliff, *Thèse de Magister*, INA, Alger, Algérie, 138 p.

Saidi, D.; Douaoui, A.; Le Bissonnais, Y. and Walter, C. (1999): Sensibilité de la surface des sols des plaines du Chélif à la dégradation structurale. *Etude et gestion des sols*, V. 6, No. 1, pp. 15-25.

Saidi, D.; Le Bissonnais, Y.; Duval, O.; Daoud, Y. and Halitim, A. (2004): Effet du sodium échangeable et de la concentration saline sur les propriétés physiques des sols de la plaine du Cheliff (Algérie). *Etude et gestion des sols*, V. 11, No. 2, pp. 137-148.

Saidi, D. (2005): Influence de la phase saline sur les propriétés physiques des matériaux argileux du Bas Cheliff. Thèse de Doctorat d'Etat, INA, Alger, 190 p.

Shainberg, I.; Oster, J. D. and Wood, J. D. (1980): Sodium/calcium exchange in montmorillonite and illite suspensions. *Soil Sci. Soc. Am. J.*, V. 44, pp. 960-964.

Shainberg, I. and Letey, J. (1984): Response of soil to sodic and saline conditions. *Hilgardia*, V.52 (2), pp. 1- 57.

Stengel, P. (1979): Utilisation de l'anaIyse des systèmes de porosité pour la caractérisation de l'état physique du sol in situ, *Ann. Agron.,* V. 30 (1), pp. 27-5.

Stengel, P. and Bourlet, M. (1987): Fissuration d'un sol argileux gonflant après compactage : Effet de l'humectation. In : Soil compaction and regeneration. Proc Workshop Soil Compaction: Consequ-ences and structural regeneration processes Avignon (France, 1985) (G Monnier, MJ Goss, Eds), Balkema, Rotterdam, pp. 95-110.

Tessier, D. and Berrier, J. (1979): Utilisation de la microscopie électronique à balayage dans l'étude des sols. Observations des sols humides soumis à différents pF. *Sciences du Sol*, 8p.

Tessier, D. (1981): Hydric behaviour and fabric of Ca and Na smectites. Conférences argiles, Etats de l'eau. Versailles 7 p.

Tessier, D. (1984): Etude expérimentale de l'organisation des matériaux argileux. Hydratation, gonflement et saturation au cours de la dessiccation et de la réhumectation. *Thèse Doctorat. Ès Sciences*, Université de Paris, VII, 361 p.

Vachier, P.; Cambier, P. and Prost, R. (1979): Structure d'un milieu poreux : la craie, Ann. Agron., V. 30, pp. 247-263.

Valentin, C. (1981): Organisation pelliculaires superficielles de quelques sols de la région subdésertique (AGADEZ, République du Niger). Dynamique de formation et conséquences sur l'économie en eau. Thèse de Doctorat, Université, Paris VI, 259 p.

Yousaf, M.; Ali, O. M. and Rhoades, J. D. (1987): Clay dispersion and hydraulic conductivity of some salt-affected arid land soil. *Soil Sci. Soc. Am. J.,* V. 51, pp. 843-854.

تأثيرات الملوحة على مسامية التربةَ في وادى الشليف بالجزائر

جمال سعيدى * ، يوسف داوود ** ، محمود أحمد عيسي ***

*كلية العلوم الزراعية والبيولوجية – جامعة شليف – الجزائر

** قسم علوم التربة بمركز الحراش – الجزائر

*** قسم الجيولوجيا – كلية العلوم – جامعة أسيوط – مصر

تمت دراسةَقلافَلت مسامية التربة الطينية الملحية والصودية باستخدام عِ دَّ ة طرق مختلفة منها مسامية الزئبقِ والتسرَّ بَ النهائي للمياه وحصر المياه والفحص الميكروسكوبى. وقد أوضحت النتائج الرئيسية أن الملوحة الشديدة يصاحبها زيادة فى الحجم الكلى للفراغات البينية بين حبيبات التربة. حيث بينت الدراسة أن درجة تركيز الملوحة الناتج عن نسبة تبادل الصوديوم (ESP) بقيمة تصل إلى 25.5% تسبب زيادة فى الحجم الكلى للفراغات بنسب تصل إلى 63.4%.

وقد أوضحت منحنيات توزيع أقطار الفراغات البينية وجود ثلاثة أنواع من أحجام الفراغات البينية (المسامية) متمثلة بمسامية هيكلية وثغرية وطينية. وقد وجد أن كلا من المسامية الهيكلية والثغرية مرتبطتان خطيا بنسبة التبادل الصوديومى (ESP) وعلى النقيض من ذلك فإن المسامية الطينية تقل بزيادة درجة ملوحة التربة. وقد أوضحت نتائج تأثير نسبة التبادل الصوديومى على حجم الفراغات البينية فى التربة أن نسب التبادل الصوديومى الأقل من 11% تؤدى إلى زيادة الفراغات البينية فى المسامية الطينية بنسبة أعلى منها فى المسامية الهيكلية والثغرية على التوالى. وعلى العكس من ذلك فإن نسب التبادل الصوديومى الأعلى من 11% تؤدى إلى زيادة الفراغات البينية فى المسامية الهيكلية والثغرية بنسبة أعلى منها فى المسامية الطينية. وقد ساهم الفحص المجهرى لقطاعات التربة الرقيقة فى معرفة التراكيب الدقيقة ومعرفة الأنواع المختلفة للمسامية بها. وقد أوضحت الدراسة أن نسبة المواد الطينية هى الأكثر شيوعاً ، وأن حجم الفراغات البينية بين حبيباتها أقل من غيرها، ويعزى ذلك إلى دور الصوديوم الذى يؤدى إلى زيادة أسطح الأتصال بين حبيبات الطين مما يؤدى إلى نقصان الفراغات البينية بينها.